Journal of Applied Electrochemistry **34**: 953–961, 2004.

Effects of temperature and concentration on the structure and specific capacitance of manganese oxide deposited in manganese acetate solution

J.-K. CHANG and W.-T. TSAI*
Department of Materials Science and Engineering, National Cheng Kung University, Tainan, Taiwan
*(*author for correspondence, fax: +886 6 2754395, e-mail: wttsai@mail.ncku.edu.tw)*

Received 19 August 2003; accepted in revised form 10 May 2004

Key words: anodic deposition, electrochemical property, manganese oxide, pseudocapacitor

Abstract

The deposition of manganese oxide on a carbon substrate in manganese acetate solution by anodic deposition was investigated. The effects of electrolyte concentration (0.05–1 M) and temperature (0–50 °C) on the characteristics of the oxide prepared were explored. The surface morphology of the oxide deposited was examined by scanning electron microscopy (SEM). Oxide whiskers were found on the deposited film surface, and they became coarser and longer when deposited at a high temperature. X-ray photoelectron spectroscopy (XPS) was carried out to examine the composition of the deposit. The results indicated that the oxides deposited at 0 and 25 °C contained trivalent and tetravalent manganese oxide. However, the mixture of bivalent and trivalent oxide was found when the deposition temperature was raised to 50 °C. Moreover, the amount of anhydrous Mn oxide (i.e., Mn–O–Mn) and water content in the deposit gradually decreased with increasing deposition temperature. The concentration of manganese acetate could affect the oxidation state of manganese ions as well as the morphology of the oxide deposited. Cyclic voltammetry (CV) was used to evaluate the electrochemical performance of the oxide deposited. The results showed that the specific capacitance of the manganese oxide increased with decreasing deposition temperature. Moreover, an optimum value of specific capacitance was found for the oxide deposited in 0.5 M manganese acetate solution.

1. Introduction

Electrochemical capacitors are charge-storage devices that possess high power density, exhibit excellent reversibility, and have very long cycle life [1]. They have recently attracted much attention in many fields (e.g., hybrid power sources, peak power sources, backup power storage, lightweight electronic fuses, starting power of fuel cells) [2–4]. Energy storage mechanisms for electrochemical capacitors include the separation of charges at the interface between a solid electrode and an electrolyte [5–7], and/or fast, continuous, and reversible faradic reactions occurring near an electrode surface over an appropriate range of potentials [2, 8–10]. The capacitance corresponding to the former mechanism is generally called double-layer capacitance. The capacitance resulting from the latter mechanism is often called pseudocapacitance. Because of the involvement of the electrochemical redox reaction of the electrode material, the capacitance per unit area given by the latter mechanism is much higher than that of the former. The most famous material exhibiting a high specific capacitance for pseudocapacitor application is ruthenium oxide. Although amorphous hydrous ruthenium oxide prepared by the sol–gel process exhibits ideal pseudo-capacitive behaviour, with a very large specific capacitance (over 700 $F\,g^{-1}$) and excellent reversibility [8, 9], the high cost of the material has limited its commercial use. Therefore, the search for a cheaper oxide with equivalent characteristics is attracting attention.

The natural abundance of manganese oxide and its environmental compatibility make it a promising electrode material for use in various energy-storage technologies. Recently, several researchers have begun to develop an effective method for preparing manganese oxide with favorable pseudo-capacitive characteristics [11–13]. In our previous work [14], the hydrous manganese oxide with ideal pseudo-capacitive behaviour was successfully prepared on a carbon substrate by anodic deposition in manganese acetate solution. The results indicated that the material characteristics and consequently the specific capacitance of the deposited oxide strongly depend on the deposition potential. Whether the deposition temperature and concentration of manganese acetate affect the material properties and capacitive behaviour of manganese oxide is of interest and is investigated in this study.

2. Experimental details

Manganese oxide was electroplated onto 1 cm × 1 cm carbon substrates by anodic deposition in manganese acetate ($Mn(CH_3COO)_2{\cdot}4\,H_2O$) plating solution. The anodic potential of 0.5 V vs SCE was adopted for oxide deposition since porous and multivalent manganese oxide with satisfactory specific capacitance could be obtained as reported in a previous study [14]. The temperature of the electrolyte was 0, 25 and 50 °C, and the concentration was varied from 0.05 to 1 M. The substrates were first polished with SiC paper of grit 800, degreased with acetone and water, then cleaned in a 25 °C 0.2 M H_2SO_4 solution, and finally washed with pure water in an ultrasonic bath. During the deposition, the carbon substrate was held as the anode and a platinum sheet was used as the counter electrode. A saturated calomel electrode (SCE) was used as the reference electrode. An EG&G Princeton Applied Research model 263 potentiostat was employed to control the deposition conditions. Anodic deposition was performed under a constant applied potential of 0.5 V vs SCE. The total passed charge during the deposition was 1.5 coulombs for each electrode. After deposition, the electrode was dried in air at room temperature. The amount of manganese oxide loaded onto the carbon substrate was then weighed in a microbalance with an accuracy of 10 μg.

The crystal structure of the manganese oxide deposited at various anodic potentials was determined by X-ray diffraction. The patterns were recorded on a Rigaku D/MAX2500 diffractometer with a glancing incident angle of 0.5°. The $K\alpha_1$ radiation of a copper target with a wavelength of 154 pm (1.540 56 Å) was used as the X-ray source. The detected diffraction angle (2θ) was scanned from 20° to 80° with a speed of 4° per minute. The surface and cross-section morphologies of the prepared manganese oxides were observed with a scanning electron microscope (SEM, Philip XL-40FEG). X-ray photoelectron spectroscopy (XPS) was also carried out to evaluate the chemical state of the manganese oxide deposited at various conditions. The measurements were performed with an ESCA 210 (VG Science Ltd) spectrometer. Monochromated Al $K\alpha$ (1486.6 eV) radiation was utilized as the X-ray source. The pressure in the analysing chamber was approximately 1×10^{-9} torr during the measurements.

The electrochemistry of the manganese oxide was characterized by cyclic voltammetry (CV) in 2 M KCl solution at room temperature. The test cell was a three-electrode system in which the manganese oxide electrode was assembled as the working electrode. A platinum sheet and a saturated calomel electrode (SCE) were used as the counter electrode and the reference electrode, respectively. The measuring instrument was also an EG & G M263 potentiostat. The potential was cycled within a potential range of 0–1 V vs SCE with a scanning rate of 5 mV s^{-1}.

3. Results and discussion

3.1. *Effect of deposition temperature*

The manganese oxides were deposited in 0.5 M manganese acetate solution at an anodic potential of 0.5 V vs SCE at various temperatures (0, 25 and 50 °C), and their material characteristics and electrochemical properties were studied. For a total anodic charge of 1.5 C, the time required to deposit the manganese oxide decreased significantly as the deposition temperature was raised. The variations of deposition current with time at different temperatures are depicted in Figure 1. It took 5834, 1107 and 237 s to deposit the oxide at 0, 25 and 50 °C, respectively.

The crystal structures of the deposited manganese oxides were examined by glancing angle XRD. Figure 2 gives an example of the diffraction pattern of the anodized oxide deposited in 0.5 M manganese acetate solution at 50 °C. The pattern includes two broadened peaks at 37.1° and 65.3°, similar to that of manganese oxide powder synthesized by Jeong and Manthiram [15]. The result indicates that the manganese oxide prepared had poor crystallinity and/or very fine grains. The diffraction patterns of the oxide deposited at 0 °C and 25 °C were similar to that demonstrated in Figure 2.

The surface morphologies of the manganese oxides, deposited in 0.5 M manganese acetate solution at 0.5 V vs SCE, were examined by SEM. The micrographs shown in Figure 3 illustrate the appearance of the oxide deposited at various temperatures. Cracks and granular oxide were seen on the surface of the electrode prepared at 0 °C (Figure 3(a)). In fact, at a low magnification, the surface morphologies of all manganese oxides deposited at different temperatures were almost the same. At high magnification, however, the SEM micrographs (Figures

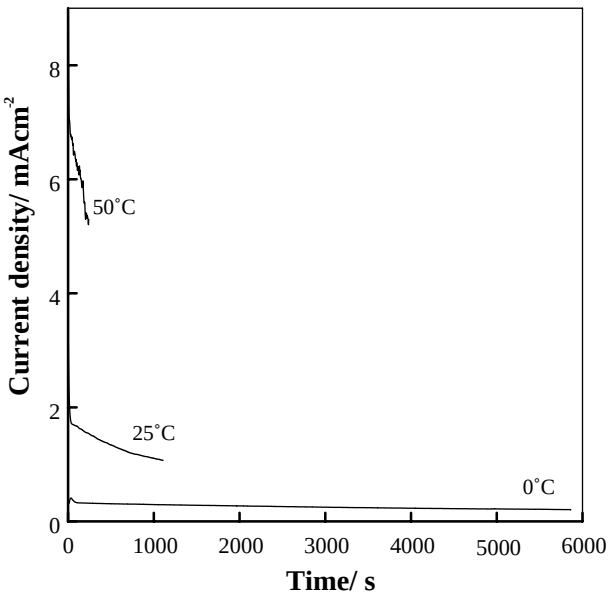

Fig. 1. Variation of deposition current with time at different temperatures in 0.5 M manganese acetate solution.

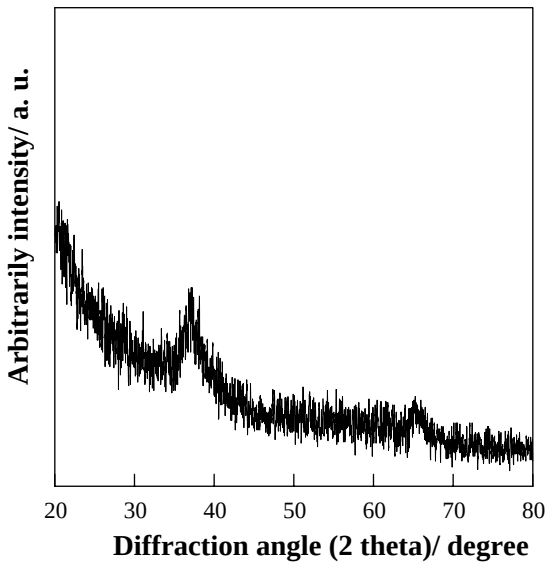

Fig. 2. Diffraction pattern of the manganese oxide deposited in 0.5 M manganese acetate solution at 50 °C.

3(b)–(d)) revealed different surface appearances. The electrode surfaces were covered with oxide whiskers which became coarser and longer as the deposition temperature increased. Figure 4 shows the typical SEM cross-section morphology of the manganese oxide deposited at 25 °C in 0.5 M manganese acetate solution at an anodic potential of 0.5 V vs SCE. The thickness of the oxide layer was about 3.5 μm. The SEM micrograph at high magnification, shown in Figure 4(b), reveals the highly porous structure of the oxide. The cross sections of the manganese oxides deposited at various temperatures exhibited the porous structure similar to that shown in Figure 4.

Figure 5 shows XPS spectra of the Mn $2p_{3/2}$ orbit for the manganese oxide deposited at various temperatures. The broadened peaks imply that the deposited oxide contained a multivalent state of manganese ions. Although it is not easy to differentiate the valence states of Mn ions from this XPS spectrum, a shift in binding energy of the Mn $2p_{3/2}$ electron for the oxides deposited at different temperatures is noticed. As indicated in Figure 5, the peaks for Mn $2p_{3/2}$ electron located at 642.6, 642.4 and 642.2 eV for the oxides deposited at 0, 25 and 50 °C, respectively. Since the higher oxidation state of the manganese in the oxide gives a higher binding energy of the Mn $2p_{3/2}$ electron [16, 17], the analytic results obtained in this investigation suggested that the relative amount of Mn ions with different oxidation states varied with deposition temperature. More specifically, the amount of Mn ion with a higher oxidation state increased with decreasing deposition temperature. Moreover, the differentiation of the chemical state of deposited manganese oxides can also be resolved by investigating the multiplet splitting width of Mn 3s peaks and the corresponding O 1s spectra [18, 19]. The exchange interaction between the core level electron (3s) and the unpaired electrons in the valence band level (3d) results in the peak separation of the Mn 3s spectrum upon photoelectron ejection [20–22]. Accordingly, the lower valence of manganese gives rises to wider splitting of the 3s peaks. Figure 6 shows XPS spectra of the Mn 3s orbit for the manganese oxide deposited at various temperatures. Clearly, the peak separation (ΔE) of Mn 3s spectra increased with increasing temperature. The Gauss fittings corresponding to the results of Figure 6 are listed in Table 1. The multiplet splittings of Mn 3s for MnO, Mn_3O_4, Mn_2O_3

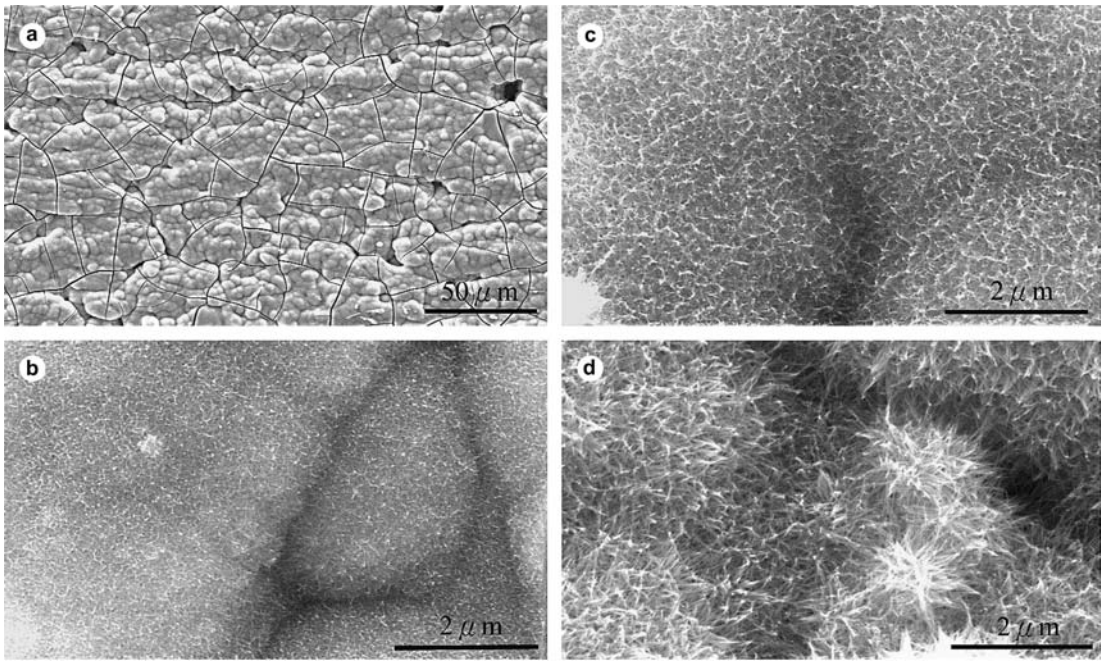

Fig. 3. SEM micrographs with different magnification showing the surface morphologies of the manganese oxide deposited at various temperature; (a, b) 0 °C, (c) 25 °C and (d) 50 °C. (Anodized at 0.5 V vs SCE in 0.5 M manganese acetate solution.)

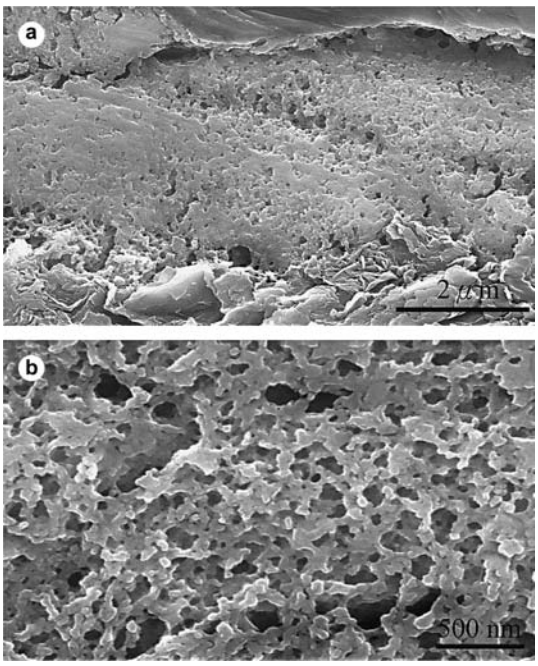

Fig. 4. SEM cross-section micrographs of the manganese oxide deposited at 25 °C in 0.5 M manganese acetate solution with different magnifications. (Anodic potential 0.5 V vs SCE.)

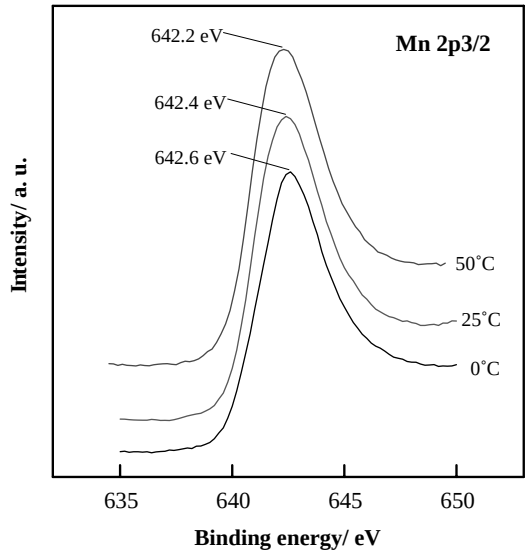

Fig. 5. XPS spectra of the Mn $2p_{3/2}$ orbit for the manganese oxide deposited at 0, 25 and 50 °C, respectively. (Anodized at 0.5 V vs SCE in 0.5 M manganese acetate solution.)

and MnO_2 have been reported by Chigane and Ishikawa [18], also listed in Table 1. The results obtained in this investigation suggest that the oxides deposited at 0 and 25 °C consisted of a mixture of trivalent and tetravalent Mn ions while the oxide deposited at 50 °C contained predominantly a mixture of bivalent and trivalent Mn ions. The poor crystallinity (shown in XRD patterns) and wide variation of oxidation state of the deposited manganese oxides suggested that they were non-stoichiometric in nature. Clearly, the average valence state of

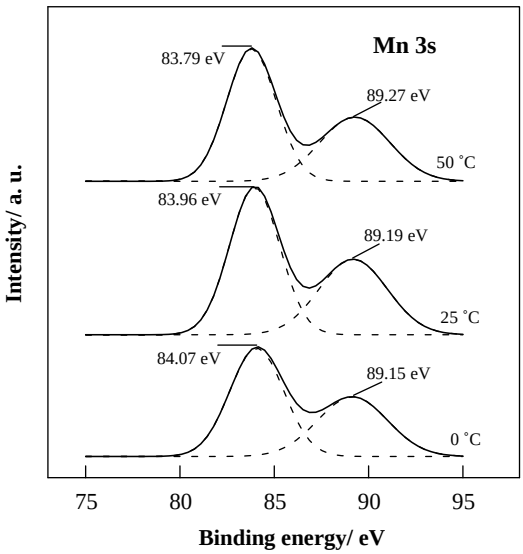

Fig. 6. XPS spectra of the Mn 3s orbit for the manganese oxide deposited at 0, 25 and 50 °C, respectively. (Anodized at 0.5 V vs SCE in 0.5 M manganese acetate solution.)

Table 1. XPS Mn 3s analytical results of manganese oxides deposited in 0.5 M manganese acetate solution at various temperatures, and in different concentrations of manganese acetate solution at 25 °C

	E_{b1} / eV	E_{b2} / eV	ΔE /eV	Species [18]
0 °C, 0.5 M	84.07	89.15	5.08	
25 °C, 0.5 M	83.96	89.19	5.23	
50 °C, 0.5 M	83.79	89.27	5.48	
25 °C, 0.05 M	84.10	89.13	5.03	
25 °C, 0.25 M	83.97	89.16	5.19	
25 °C, 0.75 M	83.98	89.16	5.18	
25 °C, 1.00 M	84.01	89.15	5.14	
	83.37	89.16	5.79	MnO
	83.36	88.86	5.50	Mn_3O_4
	83.36	88.77	5.41	Mn_2O_3
	83.92	88.7	4.78	MnO_2

Mn in the manganese oxide decreased with increasing deposition temperature.

The O 1s spectra of the manganese oxides deposited at various temperatures were further analyzed with the results presented in Figure 7. The spectra obtained could be deconvoluted into three constituents corresponding to different oxygen-containing species such as oxide (Mn–O–Mn) at 529.3–530.3 eV, hydroxide (Mn–O–H) at 530.5–531.5 eV and water molecule (H–O–H) at 531.8–532.8 eV [18, 19]. The areas under the peaks (measured in percentage under O 1s peak) of these three species for the oxides deposited at different temperatures are summarized in Table 2. A higher percentage area indicates a higher amount of the corresponding species in the oxide. By raising the deposition temperature, the amounts of anhydrous Mn oxide (i.e., Mn–O–Mn) and water content decreased gradually. But a noticeable increase in the intensity of the manganese hydroxide (i.e., Mn–O–H) was observed when the deposition

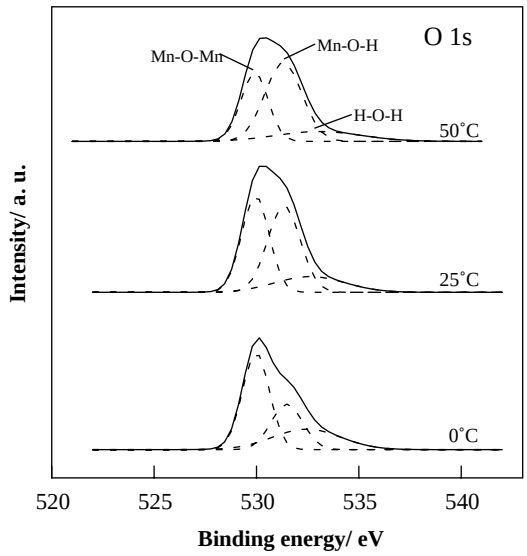

Fig. 7. XPS spectra of the O 1s orbit for the manganese oxide deposited at 0, 25 and 50 °C, respectively. (Anodized at 0.5 V vs SCE in 0.5 M manganese acetate solution.)

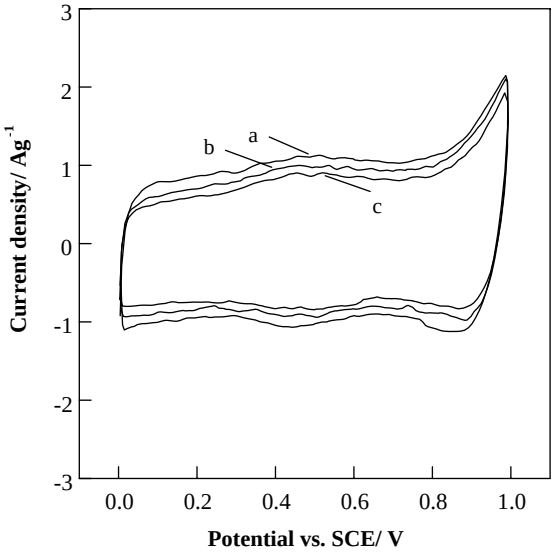

Fig. 8. Cyclic voltammograms of the manganese oxide electrodes deposited at (a) 0, (b) 25 and (c) 50 °C. (Measured in 2 M KCl solution at 25 °C, with a potential scanning rate of 5 mV s^{-1}.)

Table 2. XPS O 1s analytical results of manganese oxides deposited in 0.5 M manganese acetate solution at various temperature, and in different concentration of manganese acetate solution at 25 °C

	O 1s	
	Species	Area (%)
0 °C, 0.5 M	Mn–O–Mn	48
	Mn–O–H	26
	H–O–H	26
25 °C, 0.5 M	Mn–O–Mn	40
	Mn–O–H	40
	H–O–H	20
50 °C, 0.5 M	Mn–O–Mn	33
	Mn–O–H	52
	H–O–H	17
25 °C, 0.05 M	Mn–O–Mn	58
	Mn–O–H	20
	H–O–H	22
25 °C, 0.25 M	Mn–O–Mn	45
	Mn–O–H	34
	H–O–H	21
25 °C, 0.75 M	Mn–O–Mn	45
	Mn–O–H	35
	H–O–H	20
25 °C, 1 M	Mn–O–Mn	48
	Mn–O–H	31
	H–O–H	21

temperature was increased. The results indicated that the formation of manganese hydroxide was favoured at a high deposition temperature.

Figure 8 shows the cyclic voltammograms of various manganese oxide electrodes measured in 2 M KCl solution at 25 °C, with a potential scanning rate of 5 mV s^{-1}. Within the potential range 0–1 V vs SCE, the capacitive-like and symmetric i/E responses of the CV curves indicated that the oxides deposited at different temperatures exhibit electrochemical characteristics suitable for pseudocapacitor application. Moreover, since the voltammetric charge on the positive and negative sweeps were approximately equal, the reversibility of the redox transitions in each deposited manganese oxide was very high. However, the specific voltammetric charge (voltammetric charge per gram of the deposited manganese oxide), integrated from positive to negative sweeps, varied with the deposition temperature. The size of the rectangular loop, which reveals the capability of charge storage, decreased with increasing deposition temperature. The specific capacitance (C) of the manganese oxide could be evaluated from Equation 1:

$$C = \frac{\text{specific voltammetric charge}}{\text{potential range}} \quad (1)$$

The calculated specific capacitance values of the manganese oxide, measured in 2 M KCl solution with a potential scanning rate of 5 mV s^{-1}, are 230, 210 and 185 F g^{-1} for those deposited at 0, 25 and 50 °C, respectively. The higher specific capacitance of the manganese oxide deposited in 0.5 M manganese acetate solution at lower temperature can be attributed to the change of oxidation state of Mn ion, the variation of the hydrous state of the oxide and the difference in the fineness of the surface microstructure as demonstrated in the high magnification SEM micrographs (in Figure 3).

3.2. *Effect of solution concentration*

The effect of manganese acetate concentration, in the range 0.05 to 1 M, on the properties of the deposited oxide electrode was further investigated. For a total anodic charge of 1.5 C, the time required to deposit the manganese oxide at an applied potential of 0.5 V vs SCE varied not only with the deposition temperature but also

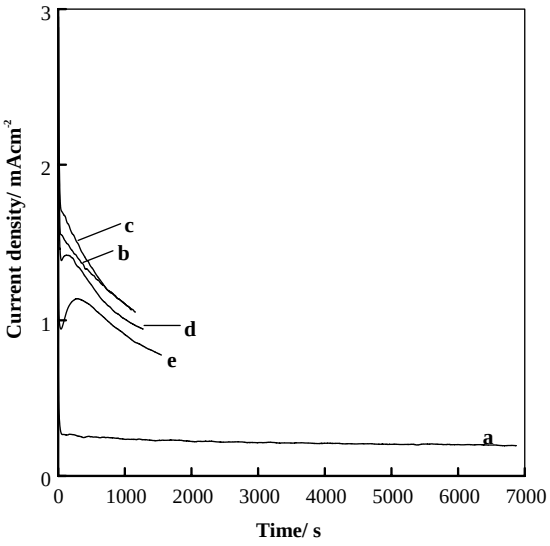

Fig. 9. Variation of deposition current with time at different concentration of the plating electrolyte at 25 °C; (a) 0.05, (b) 0.25, (c) 0.5, (d) 0.75 and (e) 1 M.

with the concentration of the plating solution. At 25 °C, the variations of deposition current with time in the solutions with different concentrations are depicted in Figure 9. The anodic current for electrode deposited in the manganese acetate solution at a concentration of 0.5 M was the highest. The times required for constant charge (1.5 C) deposition are summarized in Table 3. The deposition time did not decrease monotonously with concentration of the plating solution. The highest oxide deposition rate was found in the plating solution with 0.5 M manganese acetate, regardless of the deposition temperature.

The crystal structures of the manganese oxides deposited in solutions with various concentrations were examined by XRD. Two broadened peaks at 37.1° and 65.3° were found in the diffraction pattern of each oxide, similar to that shown in Figure 2. Figure 10 shows the SEM micrographs of the oxide electrodes deposited in manganese acetate solution with the concentration varied from 0.05 to 1 M. Clearly, the variation of manganese acetate concentration affected the surface morphology of the oxide deposited. The smooth surface of the oxide with loose structure was observed at 0.05 M. As the concentration was raised to 0.5 M, a more

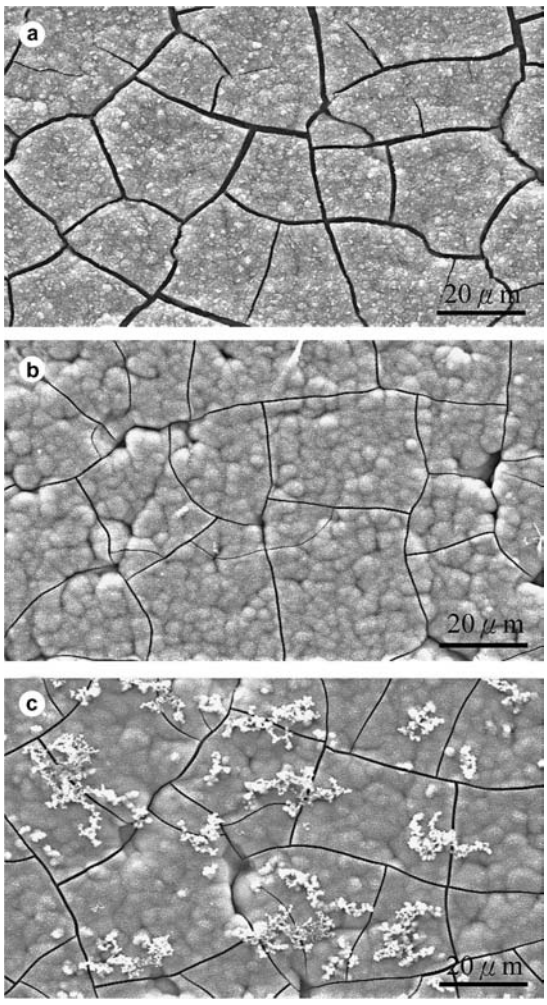

Fig. 10. Surface morphologies of the manganese oxide deposited in (a) 0.05, (b) 0.5 and (c) 1 M manganese acetate solution. (Anodized at 0.5 V vs SCE and 25 °C.)

compact oxide with granular surface was seen. There were many nodules on the oxide surface as the concentration of manganese acetate was further increased. According to EDS analysis, the oxide nodules, presented in Figure 10(c), had an O/Mn content ratio about 20% higher than that of the other region. This implies that the oxide nodules may have the highest oxidation state of Mn ions. Moreover, the difference in surface appearance of the oxides deposited in different plating solutions was further recognized by examining the SEM

Table 3. Effects of deposition temperature and solution concentration on the deposition time and specific capacitance of the manganese oxides deposited at 0.5 V vs SCE in 0.5 M manganese acetate solution

Concentration	0 °C		25 °C		50 °C	
/M	Deposition time /s	Specific capacitance /F g^{-1}	Deposition time /s	Specific capacitance /F g^{-1}	deposition time /s	specific capacitance /F g^{-1}
0.05 M	24 907	174	6875	150	1084	140
0.25 M	6887	201	1157	191	312	176
0.5 M	5834	230	1107	210	237	185
0.75 M	9032	193	1273	180	253	167
1 M	10 486	183	1548	171	474	160

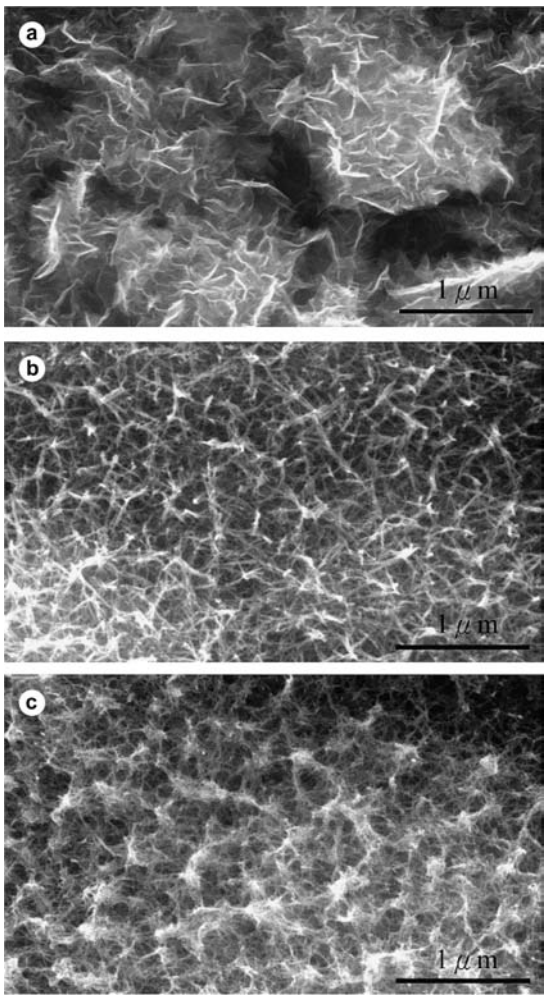

Fig. 11. SEM micrographs of the manganese oxide deposited in (a) 0.05, (b) 0.5 and (c) 1 M manganese acetate solution. (Anodized at 0.5 V vs SCE and 25 °C.)

micrographs under higher magnification (Figure 11). The surfaces were covered with oxide fibers or whiskers. The diameters of these fibers were of nanometer order and decreased as the concentration of manganese acetate increased from 0.05 to 1 M, deposited at 25 °C at a potential of 0.5 V vs SCE. The fibres on the surface formed either in 0.5 or 1 M manganese acetate solution exhibited an interwoven network (Figure 11(b) and (c)), in contrast to that of the less continuous and non-uniform deposit as formed in 0.05 M manganese acetate solution (Figure 11(a)). The oxide whiskers became finer and tangled as the concentration of the manganese acetate was raised to 1 M.

The compositions of oxides deposited in different concentrations of manganese acetate solution at 25 °C were also examined by XPS. The spectra of Mn 3s and O1s orbits were similar to those shown in Figures 6 and 7. The results are also included in Table 1 and 2. The multiplet splitting width of the Mn 3s electron and the peak ratio of Mn–O–Mn to Mn–O–H as a function of manganese acetate concentration are demonstrated in Figure 12. The separation of the split Mn 3s peaks is within the range 5.03–5.14 eV, indicating that the

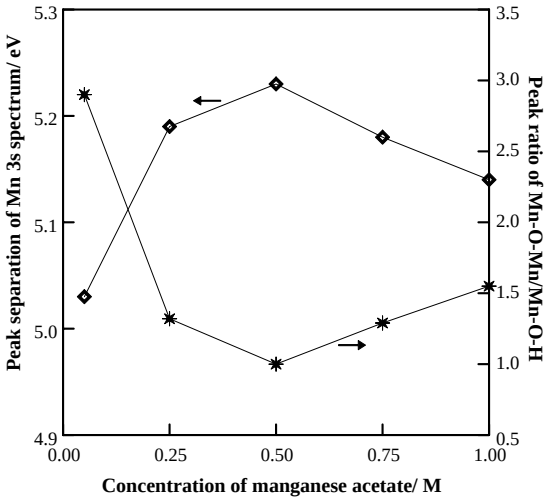

Fig. 12. XPS results showing the effect of manganese acetate concentration on the peak separation of Mn 3s spectrum and the peak ratio of Mn–O–Mn/Mn–O–H for the oxides deposited at 25 °C.

deposits were mixtures of trivalent and tetravalent manganese oxide [18]. The widest peak separation of the Mn 3s spectrum was found for the oxide formed in 0.5 M solution, suggesting it had the lowest mean oxidation state. Figure 12 also demonstrates that the oxide deposited in 0.5 M plating solution at 25 °C had the least amount of anhydrous oxide (i.e., Mn–O–Mn). Despite the change in the relative amount of hydrous and anhydrous manganese oxides, the water contents were almost constant in the oxide deposited in solutions with different manganese acetate concentration, as revealed in Table 2.

Figure 13 shows the cyclic voltammograms of manganese oxide electrodes, deposited in various solu-

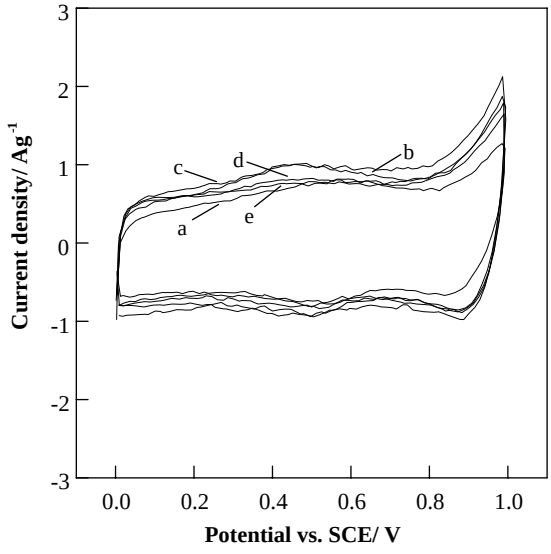

Fig. 13. Cyclic voltammograms of the manganese oxide electrodes deposited in (a) 0.05, (b) 0.25, (c) 0.5, (d) 0.75 and (e) 1 M manganese acetate solution. (Measured in 2 M KCl solution at 25 °C, with a potential scanning rate of 5 mV s^{-1}.)

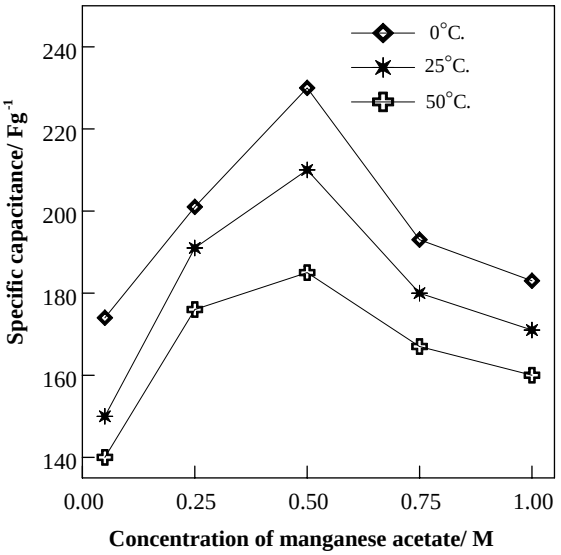

Fig. 14. Dependences of specific capacitance on solution concentration and deposition temperature.

tions at 25 °C, measured in 2 M KCl solution with a potential scanning rate of 5 mV s^{-1}. Within the potential range 0–1 V vs SCE, all electrodes exhibited excellent capacitive-like i/E responses. However, the oxide deposited in 0.5 M manganese acetate solution had the largest area CV curve. Clearly, the voltammetric charge of the manganese oxide strongly depended on the deposition conditions. The specific capacitances of the oxide electrodes deposited in various conditions are summarized in Table 3 and demonstrated in Figure 14. The specific capacitances had optimum values for the oxides deposited in 0.5 M manganese acetate solution, regardless of deposition temperature. For the oxide deposited at 0 °C, however, the specific capacitances were the highest among the oxides deposited at different temperatures. In 0.05 M electrolyte, the specific capacitance of the manganese oxide was 174 F g^{-1}, but it increased to a maximum of 230 F g^{-1} as the concentration was raised to 0.5 M. A further increase in manganese acetate concentration, however, caused the specific capacitance of the deposited manganese oxide to drop.

It is believed that the composition and surface morphology affect the electrochemical performance and the specific capacitance of the manganese oxide deposited. Both the composition and the surface morphology of the deposited oxide varied with deposition conditions. The complex dependences of specific capacitance on solution concentration and deposition temperature as revealed in Figure 14 were thus recognized. However, the specific roles of composition (such as the hydrous, anhydrous oxides and oxidation state of Mn ions) and surface morphology (such as the dimension of fibres and their distribution) on the variation of specific capacitance of manganese oxide deposited need further investigation.

4. Conclusions

Manganese oxide with promising pseudo-capacitive behaviour was prepared on a carbon substrate in manganese acetate solution by anodic deposition. The surface morphology, composition and, consequently, the specific capacitance of the oxide deposited were found to vary with the deposition temperature (0–50 °C) and the concentration (0.05–1 M) of the plating solution. The main results are summarized as follows:

(i) Oxide whiskers with diameters of nanometer scale were observed on the electrode surface. As the deposition temperature increased, they became coarser and longer. The oxidation state of the manganese ion, the amount of anhydrous Mn oxide (i.e., Mn–O–Mn) and the water content in the manganese oxide deposited gradually increased with decreasing deposition temperature.

(ii) Many oxide nodules with a higher O/Mn ratio appeared on the oxide surface as the concentration of the manganese acetate solution was raised above 0.5 M. The diameters of the oxide whiskers decreased with increasing solution concentration. Moreover, the manganese oxide deposited in the 0.5 M manganese acetate had the lowest mean oxidation state of the manganese ions and the least amount of anhydrous oxide (i.e., Mn–O–Mn).

(iii) The specific capacitance of the manganese oxide increased with decreasing deposition temperature and had an optimum value when deposited in 0.5 M manganese acetate solution at 0 °C.

Acknowledgements

The authors thank the National Science Council of the Republic of China for financially supporting this research under contract (NSC 91-2216-E-006-062).

References

1. B.E. Conway, 'Electrochemical Supercapacitors' (Kluwer–Plenum, New York, 1999).
2. B.E. Conway, *J. Electrochem. Soc.* **138** (1991) 1539.
3. S. Sarangapani, B.V. Tilak and C.P. Chen, *J. Electrochem. Soc.* **143** (1996) 3791.
4. G.L. Bullard, H.B. Sierra-Alcazar, H.L. Lee and J.L. Morris, *IEEE Trans. Magnet.* **25** (1989) 102.
5. M. Ishikawa, M. Morita, M. Ihara and Y. Matsuda, *J. Electrochem. Soc.* **141** (1994) 1730.
6. B. Pillay and J. Newman, *J. Electrochem. Soc.* **143** (1996) 1806.
7. S. Sarangapani, P. Lessner, J. Forchione, A. Griffith and A.B. Laconti, *J. Power Sources* **29** (1990) 355.
8. J.P. Zheng and T.R. Jow, *J. Electrochem. Soc.* **142** (1995) L6.
9. J.P. Zheng, P.J. Cygan and T.R. Jow, *J. Electrochem. Soc.* **142** (1995) 2699.
10. Y. Takasu, T. Nakamura, H. Ohkawauchi and Y. Murakami, *J. Electrochem. Soc.* **144** (1997) 2601.
11. H.Y. Lee, V. Manivannan and J.B. Goodenough, *Comptes Rendus Chimie* **2** (1999) 565.

12. H.Y. Lee and J.B. Goodenough, *J. Solid State Chem.* **144** (1999) 220.
13. C.C. Hu and T.W. Tsou, *Electrochem. Commun.* **4** (2002) 105.
14. J.K. Chang and W.T. Tsai, *J. Electrochem. Soc.* in press.
15. Y.U. Jeong and A. Manthiram, *J. Electrochem. Soc.* **149** (2002) A1419.
16. B.R. Strohmeier and D.M. Hercules, *J. Phys. Chem.* **88** (1984) 4922.
17. B.N. Ivanov-Emin, N.A. Nevskaya, B.E. Zaitsev and T.M. Ivanova, *Russ. J. Inorg. Chem.* **27** (1982) 1755.
18. M. Chigane and M. Ishikawa, *J. Electrochem. Soc.* **147** (2000) 2246.
19. M. Chigane, M. Ishikawa and M. Izaki, *J. Electrochem. Soc.* **148** (2001) D96.
20. D. Briggs and J.C. Riviere, *in* D. Briggs and M.P. Seah (Eds), Vol. 2, 'Practical Surface Analysis' 2nd edn (John Wiley & Sons, Chichester, UK, 1990), p. 128.
21. J.C. Carver, G.K. Schweitzer and T.A. Carlson,*J. Chem. Phys.* **57** (1972) 973.
22. M. Oku, K. Hirokawa and S. Ikeda, *J. Electron Spectrosc. Relat. Phenom.* **7** (1975) 465.